The Canadian Mineralogist
Vol. 52, pp. 235-245 (2014)
DOI: 10.3749/canmin.52.2.235

ON THE CRYSTAL-CHEMISTRY OF A NEAR-ENDMEMBER TRIPLITE, $Mn^{2+}_2(PO_4)F$, FROM THE CODERA VALLEY (SONDRIO PROVINCE, CENTRAL ALPS, ITALY)

PIETRO VIGNOLA[§]

CNR, Istituto per la dinamica dei processi ambientali, via Mario Bianco 9, 20131 Milano, Italy and Dipartimento di Scienze della Terra, Università degli Studi di Milano, via Botticelli 23, 20133 Milano, Italy

G. DIEGO GATTA

Dipartimento di Scienze della Terra, Università degli Studi di Milano, via Botticelli 23, 20133 Milano, Italy and CNR, Istituto per la dinamica dei processi ambientali, via Mario Bianco 9, 20131 Milano, Italy

FRÉDÉRIC HATERT

Laboratoire de Minéralogie, Département de Géologie, Université de Liège, Bâtiment B18, Sart Tilman, B-4000 Liège, Belgium

ALESSANDRO GUASTONI

Dipartimento di Mineralogia e Petrologia, Università di Padova, Corso Garibaldi 3735137 Padova, Italy

DANILO BERSANI

Dipartimento di Fisica, Università di Parma, Viale G.P. Usberti 7/a, 43124 Parma, Italy

ABSTRACT

The crystal-chemistry of a near-endmember triplite, a manganese fluoro-phosphate [ideal chemical formula $Mn_2(PO_4)F$; *a* 12.109(2) Å, *b* 6.5162(8) Å, *c* 10.117(1) Å, and β 106.16(2)°; space group *I* 2/*a*], from a granitic pegmatite exposed in the Codera Valley (Sondrio Province, Central Alps), has been investigated by means of wavelength dispersive electron-microprobe, infrared and Raman spectroscopies, and X-ray powder and single-crystal diffraction. Single-crystal anisotropic structure refinement gave a final agreement index $R_1 = 0.0318$ for 76 refined parameters and 1128 unique reflections with $F_o > 4\sigma(F_o)$. The structure refinement of triplite from the Codera Valley confirms the topological features previously described both for a natural sample from Mica Lode (Colorado) and for the synthetic compound $Mn_2(PO_4)F$. The structure consists of isolated PO_4 tetrahedra joined with distorted MO_4F_2 octahedra. The M(1) and M(2) octahedra share their edges to form chains; the chains of M(1) octahedra are parallel to [010], and those of M(2) are parallel to [100]. The analysis of the difference-Fourier maps of the electron density of triplite from the Codera Valley reveals a unique position for F, as reported in the literature for the OH-free synthetic $Mn_2(PO_4)F$. In contrast, two mutually exclusive F sites, with partial site occupancy, were reported in a previous structural study of OH-bearing triplite from Colorado (Mica Lode).

Keywords: triplite, granitic pegmatites, crystal structure, single-crystal X-ray diffraction, EMP chemical analyses, infrared and Raman spectroscopies.

§ *Corresponding author e-mail address*: pietro.vignola@idpa.cnr.it

Introduction

Phosphate minerals of the solid solution triplite-zwieselite, respectively $Mn^{2+}{}_2(PO_4)F$ – $Fe^{2+}{}_2(PO_4)F$, are primary phosphates commonly found in complex granitic pegmatites. These phosphates usually occur in F-rich lithium-cesium-tantalum (LCT)-type dikes, even as gigantic masses up to 4 m in diameter (Simmons *et al.* 2003).

During a field survey in the Codera Valley, Italian Central Alps, one of the authors (AG) found some masses of triplite up to 5 mm in size, hosted in a granitic pegmatite dike, and in close association with fluorapatite, Mn-bearing elbaite, and Mn oxides (Guastoni 2012). Electron-microprobe chemical analyses in wavelength-dispersive mode (EMPA-WDS) revealed a composition near to the endmember, and infrared and Raman spectroscopies confirmed the absence of OH groups. In this paper, we describe the crystal structure and crystal chemistry of this triplite sample, which was characterized by EMPA-WDS and single-crystal X-ray diffraction, as well as by infrared and Raman spectroscopies.

Background Information

Triplite was first described more than two centuries ago by Vauquelin (1802), who reported a "*phosphate natif de fer mélangé de manganèse*" from Limoges, Chanteloube, Haute-Vienne, France. Some years later, Hausmann (1813) named this new phosphate mineral "triplite". In the following two centuries, occurrences of phosphate minerals belonging to the triplite-zwieselite and triplite-triploidite solid solutions were described from a great number of granitic pegmatites, as shown by Figure 1. Among the most famous occurrences of triplite are Zwiesel, Germany (Fuchs 1839); San Luis, Sierra de Cordoba, Argentina (Stelzner 1873); Stoneham, Maine (Kunz 1884); Branchville, Connecticut (Shainin 1946); Auburn, Maine (Bastin 1911); Hagendorf, Germany (Laubman & Steinmetz 1920); Salado, La Rioja, Argentina (Henderson 1933); Mangualde, Portugal (de Jesus 1933); 7U7 Ranch and Mt Loma, Arizona (Hurlbut 1936); Varuträsk, Sweden (Mason 1941); Mica Lode and School Section, Colorado (Wolfe & Heinrich 1947); Alto do Ligonha, Mozambique (Correia Neves & Lopes Nunes 1968); Tsaobismund, Namibia (Fransolet *et al.* 1986); Okatjimukuju, Namibia (Keller & Von Knorring 1989); Fregeneda, Spain (Roda *et al.* 1996); Olary Block, South Australia (Lottermoser & Lu 1997); Cañada pegmatite, Spain (Roda *et al.* 2004).

Chemical analyses of triplite summarized by Heinrich (1951), along with those reported by other authors, show rather variable Mn:Fe:Mg ratios with different compositions belonging to the solid solution triplite-zwieselite-wagnerite. Particularly interesting is the F/OH-substitution, which appears to have a rather continuous variation in the solid-solution triplite-triploidite (Fig. 1).

The crystal structure of triplite was first solved by Waldrop (1969) using a sample from Mica Lode, Freemont County, Colorado. The chemical composition of a sample from this locality was previously reported by Heinrich (1951): $(Mn_{0.95}Fe_{0.27}Mg_{0.69}Ca_{0.08})_{\Sigma 1.99}(PO_4)(F_{0.91}OH_{0.03})_{\Sigma 0.94}$. The crystal structure was refined in space group *I*2/*a* with the following unit-cell

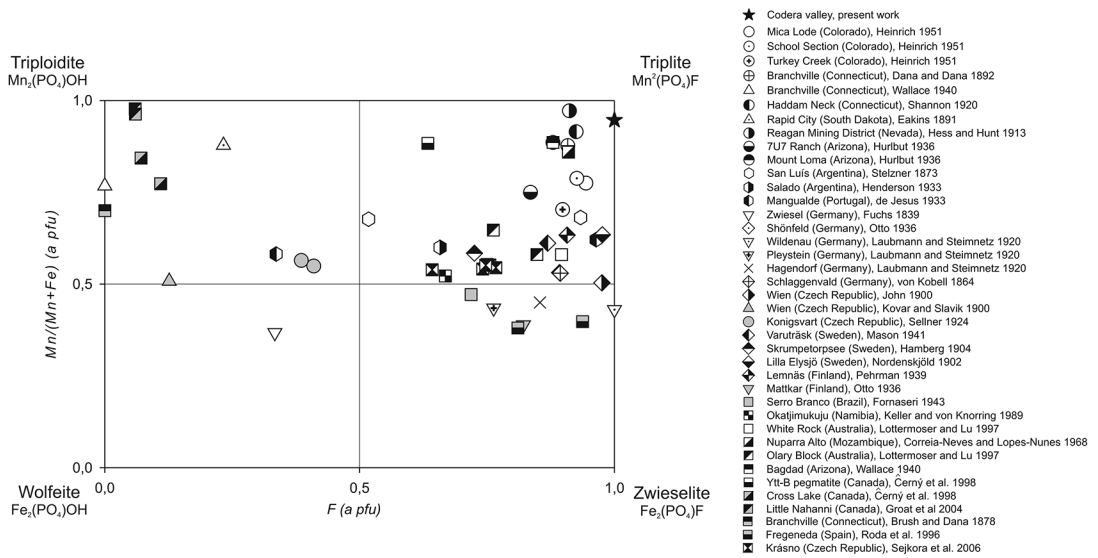

FIG. 1. F *versus* Mn/(Mn+Fe) for triplite, triploidite, wolfeite, and zwieselite reported in the literature. The star represents the triplite from the Codera Valley.

parameters: *a* 12.065(1), *b* 6.454(1), *c* 9.937(1) Å, and β 107.093(6)°. The structure is composed by isolated PO_4 tetrahedra joined on the vertices to distorted MO_4F_2 octahedra (Fig. 2). The M(1) and M(2) octahedra share their edges to form chains; the chains of M(1) octahedra are parallel to [010], and those of M(2) are parallel to [100] (Fig. 2). According to the structure model of Waldrop (1969), F is distributed between two mutually exclusive sites with partial site occupancy, located at only ~0.62 Å apart. Waldrop (1969) reported that, in the sample from Mica Lode, Mn and Fe appear to be disordered at the two octahedral sites.

Sample Description and Mineralogy

The masses of triplite were collected from a granitic pegmatite dike located in the Codera Valley (Novate Mezzola, Sondrio Province, Italy). The dike, which outcrops near the Pedroni-Dal Prà bivouac, at an elevation of 2730 m above sea level, strikes E–W with a subvertical dip . The pegmatite, hosted by the granodioritic unit of the Màsino-Bregaglia pluton (Schmid *et al*. 1996), consists of K-feldspar, quartz and plagioclase with muscovite, garnet, biotite, tourmaline, and beryl as the main accessories. This pegmatite belongs to the Rare Element (REL-Li) type, beryl-columbite-phosphate subtype, in the classification of Peter Černý (Černý & Ercit 2005). The LCT geochemical signature is coupled with enrichment in F, as shown by the chemical composition of the phosphate minerals and elbaite. The dike is asymmetric, with zones characterized by different mineral associations. Triplite masses, up to 5 mm in diameter, occur in a zone strongly enriched in dark green to brownish yellow elbaite and colorless to pale pink beryl (Guastoni 2012). In thin section, triplite occurs as deeply fractured rounded masses; fractures are sharp and filled with Mn oxides. Under polarized light, the mineral is colorless, pleochroism is absent, and no evidence of alteration was detected. Triplite from the Codera Valley is biaxial (+) with a very high relief and anomalous interference colors up to first-order red. Tiny grains of fluorapatite occur inside the triplite masses, mainly located along fractures. Phosphate masses, hosted by feldspar, are rimmed by poly-granular quartz and albite lamellae.

Analytical Methods

Quantitative electron-microprobe analyses were obtained from a polished thin section using a JEOL JXA-8200 microprobe in wavelength-dispersive mode at the Earth Sciences Department, University of Milano (ESD-MI). The system was operated using an accelerating voltage of 15 kV, a beam current of 15 nA, a beam diameter of 5 μm, and a counting time of 30 s on the peaks and 10 s on the backgrounds. The following standards, lines and crystals were used: graftonite for P (*K*α1, PETJ), Fe (*K*α1, LIFH), Mn (*K*α1, LIFH), and Ca (*K*α1, PETH); grossular for Si (*K*α1, TAP) and Al (*K*α1, TAP); K-feldspar for K (*K*α1, PETH); forsterite for Mg (*K*α1, TAP); omphacite for Na (*K*α1, TAP); and hornblende for F (*K*α1, LDE). The raw data were corrected for matrix effects using the protocol implemented in the JEOL suite of programs.

Single-crystal X-ray diffraction data were obtained with an Xcalibur - Oxford Instruments diffractometer equipped with a CCD, using graphite-monocromatized Mo*K*α radiation, and operated at 50 kV and 40 mA at the ESD-MI. To maximize the reciprocal space coverage, a combination of ω and ϕ scans was used, with a step size of 0.5° and an exposure time per frame of 10 s. A total number of 21,608 reflections in the range $2 < 2\theta < 72.45°$ were collected, of which 1273 were unique, giving a metrically monoclinic unit-cell with *a* 12.109(2) Å, *b* 6.5162(8) Å, *c* 10.117(1) Å, β 106.16(2)°, and *V* 766.7(2) Å^3 (Table 1). Data reduction, included Lorenz-polarization and analytical absorption

TABLE 1. DETAILS PERTAINING TO THE DATA COLLECTION AND THE STRUCTURE REFINEMENT OF TRIPLITE

Crystal shape	Irregular prism
Crystal size (mm^3)	0.1 × 0.2 × 0.2
Crystal color	Transparent pink
T (K)	298
Unit-cell constants	*a* 12.109(2) Å
	b 6.5162(8) Å
	c 10.117(1) Å
	β 106.16 (2)°
	V 766.7(2) Å^3
Chemical formula	$(Mn,Fe)_2(PO_4)F$
Space Group	*I* 2/*a*
Z	8
Radiation (Å)	0.7107
Diffractometer	Xcalibur - CCD
Data-collection method	ω/φ scan
Step size	0.5°
Max. θ (°)	72.45
	$-15 < h < 16$
	$-10 < k < 10$
	$-16 < l < 16$
No. measured reflections	21,608
No. unique reflections	1273
No. unique refl. with $F_o > 4\sigma(F_o)$	1128
No. refined parameters	76
R_{int}	0.0386
Refinement on	F^2
R_1 (F) with $F_o > 4\sigma(F_o)$	0.0242
R_1 (F) for all the unique reflections	0.0318
wR_2 (F^2)	0.0432
GooF	1.698
Weighting scheme: a, *b*	0.01, 0
Residuals (*e*$^-$/ Å^3)	–0.65/+0.62

$R_{int} = \Sigma \mid F_{obs}^2 - F_{obs}^2(\text{mean}) \mid / \Sigma [F_{obs}^2]$; $R_1 = \Sigma(|F_{obs}| - |F_{calc}|)/\Sigma|F_{obs}|$; $wR_2 = [\Sigma[w(F^2_{obs} - F^2_{calc})^2]/\Sigma[w(F^2_{obs})^2]]^{0.5}$, $w = 1/[\sigma^2(F_{obs}^2) + (a*P)^2 + b*P]$, $P = (\text{Max}(F_{obs}^2, 0) + 2*F_{calc}^2)/3$

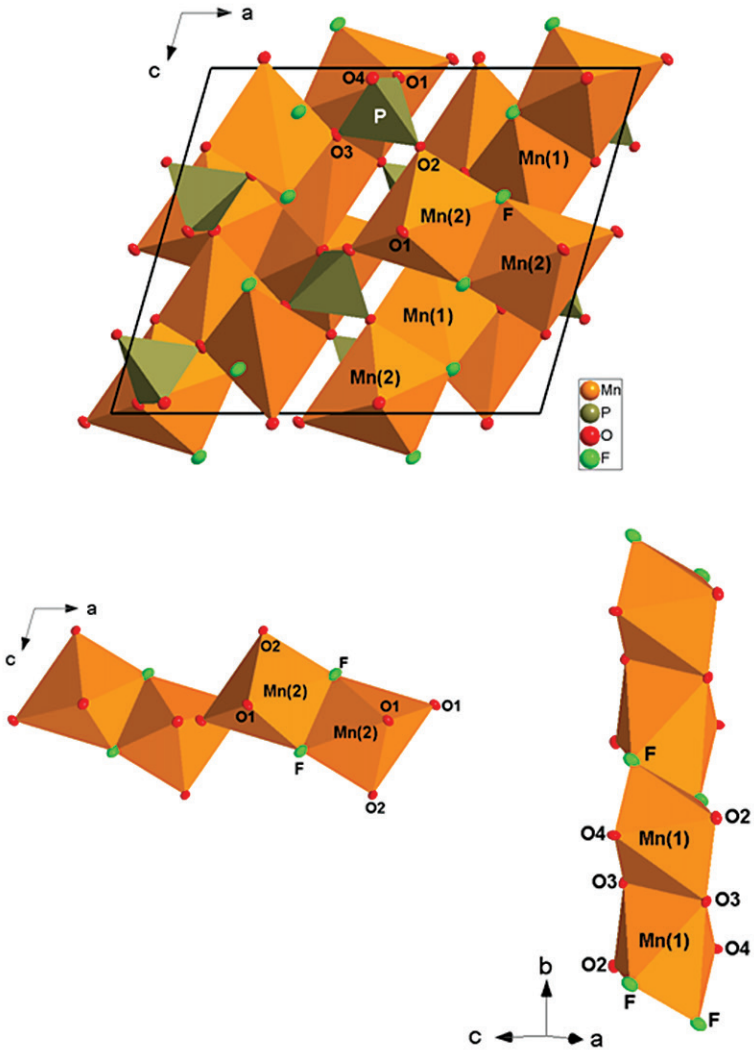

FIG. 2. The crystal structure of triplite based on the data in this study. The configuration of the M(1)-octahedral chain parallel to [010] and that of the M(2)-octahedral chains parallel to [100] are shown. The thermal ellipsoid probability factor is 50%.

correction (by Gaussian integration based upon the physical description of the crystal), were performed using the software CrysAlis (Oxford Diffraction 2010).

The X-ray powder diffraction pattern of triplite was collected using a Philips PW1710 diffractometer equipped with Cu$K\alpha$ radiation and a graphite monochromator on the diffracted beam. Operating conditions were: 40 kV, 40 mA, 2θ-range from 5 to 100°, step size of 2θ = 0.02°, counting time of 3 s per step. Silicon NIST 640c was used as an internal standard. Indexing of the diffraction pattern and refinement of the unit-cell constants was performed using the program CELREF 3 beta version (http://www.inpg.fr/LMGP). Observed and calculated interplanar distances, along with the peak intensities, are listed in Table 2.

The Raman spectrum was collected in the 100–3600 cm^{-1} region using a Jobin-Yvon Horiba Labram micro-Raman spectrometer with two different linearly polarized laser lines: 632.8 nm (He-Ne laser) and 473.2 nm (doubled Nd laser). The laser beam was focused on the sample through an Olympus microscope equipped with objectives giving up to 100× magnification. Neutral

TABLE 2. X-RAY POWDER DIFFRACTION DATA FOR THE TRIPLITE SAMPLE INVESTIGATED IN THIS STUDY. THE REFINED UNIT-CELL PARAMETERS ARE: *a* 12.133(2), *b* 6.522(1), *c* 10.129(4) Å, β 106.09(1)°

I/I_0	d_{obs} (Å)	d_{cal} (Å)	*hkl*	I/I_0	d_{obs} (Å)	d_{cal} (Å)	*hkl*
2	5.813	5.822	2 0 0	6	1.687	1.686	2 0 6
3	5.694	5.685	1 1 0	3	1.668	1.667	6 2 0
1	5.422	5.412	0 1 1	26	1.653	1.652	4 0 4
2	4.870	4.861	0 0 2	4	1.613	1.612	7 1 0
6	4.313	4.309	2 1 1	5	1.601	1.601	5 3 2
3	3.968	3.969	1 1 2	6	1.569	1.568	6 1 5
35	3.693	3.690	2 1 1	2	1.560	1.559	6 2 4
28	3.472	3.470	1 1 2	5	1.545	1.542	5 2 5
69	3.309	3.307	2 0 2	4	1.527	1.526	2 4 2
92	3.056	3.053	1 2 1	4	1.523	1.522	7 2 1
59	2.904	2.901	0 1 3	1	1.516	1.514	8 0 2
100	2.877	2.873	4 0 2	4	1.506	1.505	1 1 6
16	2.845	2.843	2 2 0	6	1.460	1.479	2 3 5
10	2.749	2.747	4 1 1	9	1.476	1.476	6 3 $\bar{1}$
8	2.709	2.706	0 2 2	5	1.461	1.461	8 1 $\bar{1}$
18	2.615	2.613	2 2 2	4	1.450	1.451	0 3 5
15	2.530	2.528	3 2 1	4	1.438	1.437	4 3 3
13	2.507	2.503	2 0 4	2	1.421	1.421	7 1 2
4	2.415	2.413	4 1 1	4	1.417	1.417	3 2 5
3	2.373	2.372	2 1 3	3	1.391	1.390	6 3 $\bar{1}$
6	2.355	2.353	1 1 4	1	1.383	1.383	4 1 $\bar{7}$
5	2.322	2.321	$\bar{2}$ 2 2	3	1.343	1.342	2 3 5
9	2.231	2.229	$\bar{5}$ 1 2	2	1.333	1.332	2 2 5
4	2.191	2.193	5 1 0	2	1.310	1.310	3 4 3
10	2.176	2.174	3 2 3	2	1.307	1.306	1 2 $\bar{7}$
5	2.157	2.155	4 2 2	1	1.295	1.296	$\bar{6}$ 3 5
8	2.134	2.135	1 3 0	3	1.248	1.248	2 5 1
21	2.121	2.119	0 3 1	3	1.242	1.241	1 5 2
22	2.052	2.050	2 0 4	2	1.233	1.233	9 2 $\bar{3}$
2	2.032	2.031	2 3 1	2	1.230	1.230	9 2 $\bar{1}$
1	2.004	2.004	6 0 2	2	1.198	1.197	6 4 $\bar{4}$
3	1.986	1.985	2 2 4	2	1.189	1.189	8 1 3
3	1.955	1.954	2 3 1	2	1.187	1.186	4 2 6
5	1.942	1.941	6 0 0	2	1.168	1.168	5 4 3
13	1.925	1.923	6 1 1	1	1.166	1.166	5 1 6
3	1.895	1.895	3 3 0	2	1.161	1.160	4 4 4
6	1.865	1.863	0 1 5	1	1.126	1.126	$\bar{7}$ 1 8
4	1.839	1.839	4 1 3	1	1.095	1.095	2 2 $\bar{5}$
11	1.826	1.826	3 2 3	1	1.086	1.086	0 6 0
12	1.818	1.816	4 2 4	1	1.082	1.080	3 4 $\bar{7}$
9	1.803	1.801	4 1 5	1	1.066	1.065	6 1 $\bar{9}$
4	1.786	1.786	5 2 1	1	1.043	1.043	9 2 3
9	1.774	1.775	3 1 4	1	1.034	1.034	1 3 8
9	1.767	1.765	4 3 1	2	1.032	1.032	2 6 2
2	1.735	1.735	2 2 4	1	1.014	1.016	5 2 7
1	1.709	1.707	6 2 2	1	1.008	1.007	4 3 7

density filters were used to minimize the laser power on the sample in order to avoid undesired heating effects. The spacial resolution was about 1 μm and the spectral resolution was set to 2 cm^{-1}.

The infrared spectrum of triplite was collected with a Nicolet NEXUS spectrometer, in the 400–4000 cm^{-1} region. Approximately 2 mg of triplite were mixed with 148 mg of KBr, crushed in an agate mortar, and maintained at 110 °C for a few hours to evacuate adsorption water. The dry mixture was then pressed to obtain a pellet of 1 cm diameter. Measurements were performed with a 1 cm^{-1} resolution, and a dry air purge was connected to the spectrometer to avoid contamination by atmospheric water and CO_2.

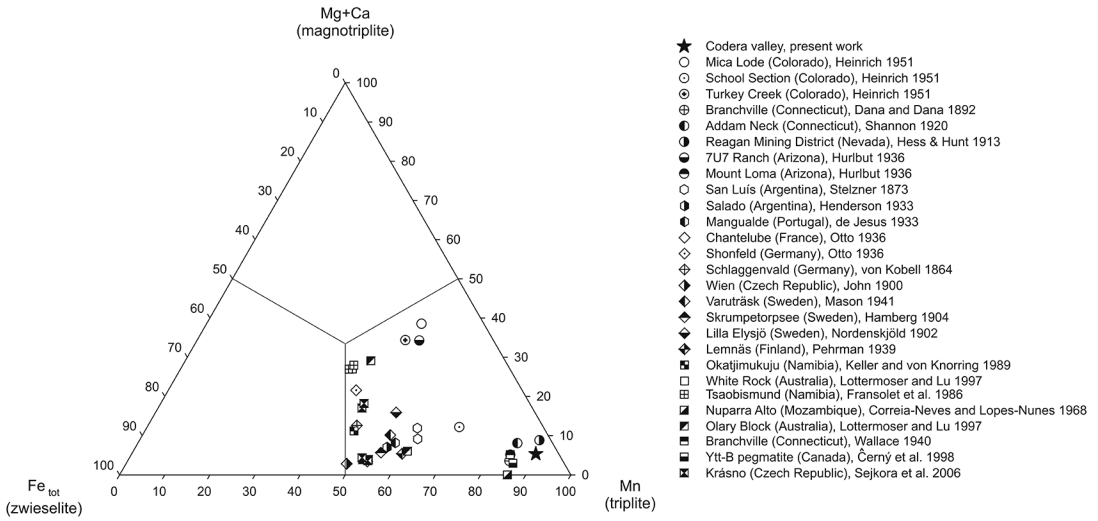

FIG. 3. Triangular (Fe)–(Mg+Ca)–(Mn) plot displaying the chemical compositions of triplite found in the literature and from this study.

TABLE 3. CHEMICAL COMPOSITION OF TRIPLITE FROM THE CODERA VALLEY (CV, THIS STUDY) AND FROM THE REAGAN MINING DISTRICT (RMD, HESS & HUNT 1913)

	CV*		RMD
	wt.%	*e.s.d.*	*wt.%*
P_2O_5	32.35	*0.15*	31.84
Al_2O_3	0.01	*0.01*	n.a.
FeO	3.27	*0.09*	1.68
MnO	56.72	*0.22*	57.63
CaO	2.51	*0.07*	2.86
MgO	0.16	*0.02*	1.21
Na_2O	0.01	*0.02*	n.a.
F	8.65	*0.05*	7.77
Σ	**103.68**		**102.99**
–O=F	–3.64		–3.27
total	**100.04**		**99.72**
	Normalized on the basis of 1 P a.p.f.u.		
P^{5+}	1.000		1.000
Al^{3+}	0.000		n.a.
Fe^{2+}	0.100		0.053
Mn^{2+}	1.754		1.811
Ca^{2+}	0.098		0.114
Mg^{2+}	0.009		0.067
Na^{+}	0.001		n.a.
F	0.999		0.912
O^{2-}	3.958		4.088

Notes: * Average of 46 analyses from 10 different grains; n.a. not analyzed

CHEMICAL COMPOSITION

The electron-microprobe composition (average of 46 analyses), obtained from 10 different grains in a thin section (Table 3), displays a high homogeneity with a maximum standard deviation of 0.22 for MnO. The divalent cation site is strongly dominated by Mn (1.754 *apfu*) followed by Fe and Ca (0.100 and 0.098 *apfu* respectively); K is below the detection limit. The amount of F, with an average value of 8.65 wt.%, corresponds to 0.999 *apfu*, indicating the absence of OH groups. A triangular (Fe)–(Mg+Ca)–(Mn) plot is shown in Figure 3, based on the compositions of triplite found in the literature and described in the present paper. Triplite from the Codera Valley plots close to the endmember composition $Mn_2(PO_4)F$, along with triplite found in a W ore from the Reagan Mining District (Aurum, White Pine Co., Nevada), which was described by Hess & Hunt (1913) (Table 3).

STRUCTURE REFINEMENT

The intensity data of triplite were first processed with the programs E-STATISTICS and ASSIGN-SPACEGROUP implemented in the WinGX package (Farrugia 1999). The statistics of distributions of the normalized structure factors suggested that the structure is centro-symmetric, and the space group *I*2/*a* as highly likely (according to the non-standard set of Waldrop 1969). The anisotropic crystal structure refinement was then performed using the SHELX-97 software (Sheldrick 1997), with starting atomic coordinates from

Waldrop (1969). Neutral scattering factors were used for Mn, P, O, and F. The secondary isotropic extinction effect was corrected according to Larson's formalism (1967), as implemented in the SHELXL-97 package (Sheldrick 1997). The scattering curve of Mn was used to model the occupancy of the octahedral M(1) and M(2) sites, leading to final site occupancies of 97.1(2)% (*i.e.*, 24.28 e^-) and 99.3(2)% (*i.e.*, 24.83 e^-) for the M(1) and M(2) sites, respectively (Table 4). After the first cycles of refinement, convergence was achieved with a structure model with only one F site (at $x \sim 0.2658$, $y \sim 0.1547$, and $z \sim 0.3728$, Table 4) with full site occupancy [*i.e.*, 99.9(5)%], rather than with two unique and mutually exclusive F sites as suggested by Waldrop (1969). At the end of the refinement, all the principal mean square atomic displacement parameters were positively defined. The final variance-covariance matrix showed no significant correlation among the refined parameters, and no peak larger than ±0.65 $e^-/Å^3$ was present in the final difference-Fourier map of the electron density (Table 1). The final agreement index (R_1) was 0.0242 for 76 refined parameters and 1128 unique reflections with $F_o > 4\sigma(F_o)$ (Table 1). Refined site coordinates and displacement parameters are reported in Table 4. Relevant bond lengths and angles are given in Table 5.

Vibrational Spectroscopies

The Raman spectra obtained from a triplite crystal using the 632.8 nm laser line is shown in Figure 4 and

TABLE 4. REFINED POSITIONAL AND ANISOTROPIC DISPLACEMENT PARAMETERS (Å^2) FOR TRIPLITE FROM THE CODERA VALLEY

Site	Site occupancy factor	*x*	*y*	*z*	U_{11}	U_{22}	U_{33}	U_{12}	U_{13}	U_{23}	U_{eq}
M1	Mn 97.1(2)%	0.19521(3)	–0.01430(4)	0.18824(3)	0.0102(2)	0.0119(1)	0.0091(1)	0.0029(1)	0.0020(1)	0.0000(1)	0.0105(1)
M2	Mn 99.3(2)%	0.09364(3)	0.14593(4)	0.44514(3)	0.0116(2)	0.0072(1)	0.0091(1)	–0.0009(1)	0.0029(1)	–0.0007(1)	0.0093(1)
P	P 100%	0.07372(5)	0.65721(7)	0.37919(5)	0.0076(3)	0.0060(2)	0.0081(2)	0.0001(2)	0.0029(2)	0.0001(1)	0.0071(1)
O1	O 100%	0.05661(14)	0.83127(18)	0.47407(14)	0.0151(9)	0.0092(6)	0.0128(6)	–0.0028(6)	0.0073(6)	–0.0032(5)	0.0117(3)
O2	O 100%	0.95951(13)	0.60809(21)	0.27198(14)	0.0090(8)	0.0165(6)	0.0099(6)	–0.00245(62)	0.0009(6)	–0.0003(5)	0.0122(3)
O3	O 100%	0.16461(13)	0.71588(20)	0.30680(14)	0.0135(9)	0.0133(6)	0.0161(7)	–0.0002(6)	0.0089(7)	0.0018(5)	0.0134(3)
O4	O 100%	0.11718(14)	0.46828(19)	0.47054(14)	0.0130(9)	0.0089(6)	0.0147(7)	0.0011(6)	0.0017(6)	0.0020(5)	0.0126(3)
F	F 99.9(5)%	0.26581(12)	0.15469(18)	0.3728(1)	0.0168(9)	0.0202(7)	0.0177(6)	0.0012(5)	–0.0011(6)	–0.0060(5)	0.0194(4)

Notes: The anisotropic displacement factor exponent takes the form: $-2\pi^2[(ha^*)^2U_{11} + \ldots + 2hka^*b^*U_{12}]$. U_{eq} is defined as one third of the trace of the orthogonalized *Uij* tensor.

TABLE 5. BOND DISTANCES (Å) AND ANGLES (°) IN THE CRYSTAL STRUCTURE OF TRIPLITE FROM THE CODERA VALLEY

P–O(1)	1.537(1)	O(1)–P–O(2)	110.10 (8)	O(4)–M(1)–F'	71.19(5)
P–O(2)	1.535(2)	O(1)–P–O(3)	110.76 (8)	F–M(1)–F'	71.04(5)
P–O(3)	1.531(1)	O(1)–P–O(4)	107.33 (8)	O(1)–M(2)–O(1)'	77.69(5)
P–O(4)	1.541(1)	O(2)–P–O(3)	109.90 (8)	O(1)–M(2)–O(2)'	90.89(5)
		O(2)–P–O(4)	110.31 (8)	O(1)–M(2)–O(4)	163.34(5)
M(1)–O (2)	2.174 (2)	O(3)–P–O(4)	108.39 (8)	O(1)–M(2)–F	107.37(5)
M(1)–O (3)	2.136 (2)	O(2)'–M(1)–O(3)	84.74(5)	O(1)–M(2)–F''	93.14(5)
M(1)–O (3)'	2.217 (1)	O(2)'–M(1)–O(3)'	160.27(5)	O(1)'–M(2)–O(2)'	110.40(6)
M(1)–O (4)	2.162 (2)	O(2)'–M(1)–O(4)'	89.02 (6)	O(1)'–M(2)–O(4)	89.15(5)
M(1)–F	2.131 (1)	O(2)'–M(1)–F	78.73(5)	O(1)'–M(2)–F	173.46(5)
M(1)–F'	2.502 (1)	O(2)'–M(1)–F'	86.20(5)	O(1)'–M(2)–F''	102.79(6)
		O(3)–M(1)–O(3)'	75.58(6)	O(2)'– M(2)–O(4)	103.39(5)
M(2)–O (1)	2.136 (1)	O(3)–M(1)–O(4)'	124.73(6)	O(2)'–M(2)–F	74.08(5)
M(2)–O (1)'	2.197 (2)	O(3)–M(1)–F	91.29(5)	O(2)'–M(2)–F''	146.67(6)
M(2)–O (2)'	2.124 (1)	O(3)–M(1)–F'	161.43(5)	O(4)–M(2)–F	85.10(5)
M(2)–O (4)'	2.126 (1)	O(3)'–M(1)–O(4)'	103.20(5)	O(4)–M(2)–F''	79.70(5)
F–M(2)	2.132 (1)	O(3)'–M(1)–F	100.07(6)	F–M(2)–F''	73.14(5)
F–M(2)'	2.395 (1)	O(3)'–M(1)–F'	112.24(5)		
		O(4)–M(1)–F	140.88(5)		

the Raman bands are summarized in Table 6. Raman measurements were collected from different points on the sample, without significant differences. Even using a different excitation wavelength (473.2 nm), similar spectra were obtained, in particular in the low-wavenumber region. The spectrum is dominated by the phosphate group vibrations. The main Raman band, which is very strong and sharp, is centered at 980.5 cm^{-1}, and can be attributed to the ν1 vibration of the phosphate unit (symmetric stretching). The bands at 1036 and 1072 cm^{-1} are due to the ν3 vibration (anti-symmetric stretching). The Raman bands in the range 300–700 cm^{-1} are essentially grouped in two regions corresponding to two different modes of the phosphate group: ν2 between 400 and 480 cm^{-1}, and ν4 between 570 and 620 cm^{-1}. Especially in this region, where many bands are present in a small spectral range, orientation effects could be important, causing the appearance or disappearance of some peaks depending on the orientation of the sample with respect to the laser polarization.

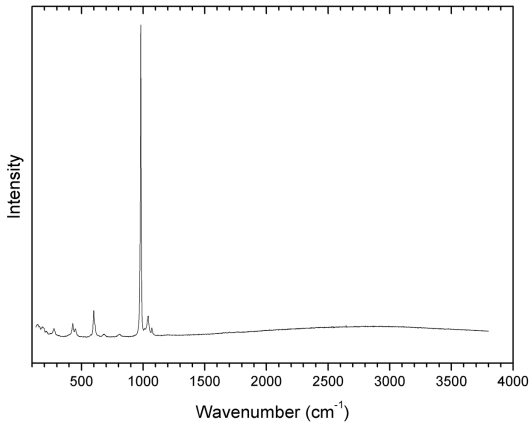

FIG. 4. Raman spectrum of triplite from the Codera Valley obtained with a 632.8 nm laser.

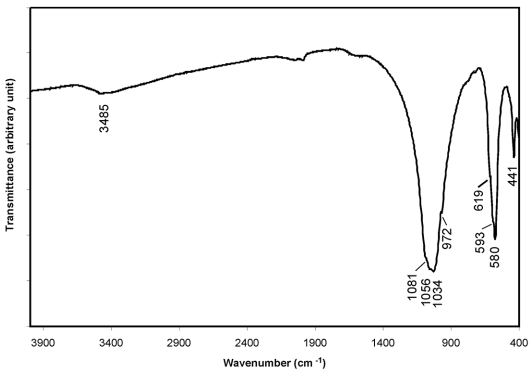

FIG. 5. The infrared spectrum of triplite from the Codera Valley.

TABLE 6. RAMAN BANDS OF TRIPLITE FROM THE CODERA VALLEY OBTAINED WITH THE 632.8 nm LASER

Raman band (cm^{-1})	Intensity	Vibration
137.5	w	lattice
161	w	lattice
179.5	w	lattice
192.5	w	lattice
218.5	w	lattice
242.5	w	lattice
277.5	w	lattice
398.5	sh	v2 ?
421	m	v2 phosphate (deform.)
429.5	sh	v2 phosphate (deform.)
450	w	v2 phosphate (deform.)
468.5	w	v2 phosphate (deform.)
573	w	v4 phosphate (deform.)
598	m	v4 phosphate (deform.)
605	m (visible in some orientation)	v4 phosphate (deform.)
610.5	m	v4 phosphate (deform.)
680	w	
807.6	w	
980.5	vs	v1 (symm. str. phosphate)
1036	m	v3 (asymm. str. phosphate)
1072	w	v3 (asymm. str. phosphate)
1120	vw (sometimes visible)	v3 ?
3498	vw	OH stretching

Below 400 cm^{-1}, the lattice modes are found. The only difference visible using a different excitation line is the presence of a very small Raman band attributed to the OH stretching modes, at 3498 cm^{-1}, visible only when using the 473.1 nm laser line. This is due to the fact that, when a blue excitation line is used, the OH stretching bands fall in a region where the apparatus is more efficient.

The infrared spectrum (Fig. 5) is characterized by the stretching vibrational modes of the PO_4 tetrahedra, which occur in the 1200–900 cm^{-1} region. The absorption bands observed between *ca.* 400 and 650 cm^{-1} correspond to the PO_4 bending vibrations, as well as to lattice vibrations. The broad absorption band, located at 3485 cm^{-1} (Fig. 5), is related to the O–H stretching vibrational mode of the OH groups. The weak intensity of this band confirms the low OH content of the investigated sample.

Discussion

The composition of the triplite sample from the Codera Valley, investigated herein, shows a relatively low amount of Fe and Mg, as well as the absence of significant OH. The IR and Raman spectra confirm the chemical composition obtained by EMPA.

The single-crystal structure refinement confirms the general model previously described by Waldrop (1969) for a natural triplite and by Rea & Kostiner (1972) for the synthetic $Mn_2(PO_4)F$ compound. The main difference with the structure model reported by Waldrop (1969) concerns the F site. Our data led to one independent F site with full site occupancy, whereas Waldrop (1969) reported two mutually exclusive F sites with partial site occupancies, located only ~0.62 Å apart, with unusually high thermal displacement parameters when compared to the other O sites. In a comparative study of the crystal structure of triplite and triploidite [*i.e.*, $(Mn,Fe)_2PO_4(OH)$], Waldrop (1970) considered the analogy of the splitting of the F site in two subsites in triplite (mutually exclusive) and that of the OH^- sites in triploidite. However, in the latter the split leads to an ordered distribution with distinct OH^- sites with full occupancies and a doubling of the cell volume (*a* 12.366, *b* 13.276, *c* 9.943 Å, β 108.23°, space group $P2_1/a$). Such a configuration appears to be ascribable to the proton-metal repulsion. Although Waldrop (1970) did not consider the possibility of a solid solution along the triplite-triploidite join, as the different F/OH environments make the structure non-isotypic, the chemical composition of triplites and triploidites reported in the literature appears to show a potential F/OH substitution (Fig. 1). Likely, the structure of triplite can preserve its metrics and symmetry (*i.e.*, *a* ~12.109 , *b* ~6.516 , *c* ~10.117 Å, β ~106.16°, space group *I*2/*a*) even with a modest F/OH substitution. Such a behavior has been observed in several F/OH-bearing minerals, in which the endmembers of the solid solutions have different symmetries [*e.g.*, topaz: $Al_2SiO_4(F,OH)_2$, Gatta *et al.* 2006a,b]. The chemical analysis of the sample of triplite used by Waldrop (1969) was performed by Heinrich (1951), and appeared to contain only a modest amount of OH [*i.e.*, $(Mn_{0.95}Fe_{0.27}Mg_{0.69}Ca_{0.08})_{\Sigma 1.99}(PO_4)(F_{0.91}OH_{0.03})_{\Sigma 0.94}$]. In their structure refinement of the synthetic $Mn_2(PO_4)F$ compound, Rea & Kostiner (1972) found only one F site, in accordance with our structural data. Only more structure refinements of crystals with compositions along the triplite–triploidite join can provide a clear picture of the role played even by a modest fraction of OH^- groups on the splitting of the (OH,F) site.

Previous structural studies suggested a highly disordered distribution of the bivalent cations among the two octahedral sites (Waldrop 1969; Keller *et al.* 1994). If we consider: (1) the modest amount of Mg and Fe, along with the pronounced amount of Ca, found in the triplite sample from the Codera Valley (Table 3) and (2) the refined site occupancy of the octahedral M(1) and M(2) sites [*i.e.*, 97.1(2)% and 99.3(2)%, respectively; Table 4], we cannot exclude the possibility that a significant amount of Ca occupies the M(1) site, along with Mn. This hypothesis is consistent with the longer M(1)–(O,F) bond distance, compared to the M(2)–(O,F) ones. In addition, our structure refinement shows a pronounced distortion of both octahedra, with $\Delta(M1–O,F)_{max}$ ~ 0.370 and $\Delta(M2–O,F)_{max}$ ~0.270 Å. In contrast, the PO_4 tetrahedron appears to be more regular, with ($\Delta(M1–O,F)_{max}$ ~ 0.011 Å).

Acknowledgments

Many thanks are due to Andrea Risplendente for his help during the electron-microprobe measurements. Radek Skoda, Fabrizio Nestola, and the Guest Editor William "Skip" B. Simmons are thanked for the revision of the manuscript. This work is part of Research Project TA.P05.020 "Processi geodinamici e pericolosità geologica: indagini interdisciplinari geologico-geofisiche" of the Istituto per la dinamica dei processi ambientali (IDPA) of the Italian National Research Council (CNR).

References

Bastin, E.S. (1911) Geology of the pegmatites and associated rocks of Maine. *United States Geological Survey Bulletin* **445**, 146.

Brush, G.B. & Dana, E.S. (1878) On a new and remarkable mineral locality in Fairfield County, Connecticut. *American Journal of Science* **16**, 33–46.

Černý, P. & Ercit, T.S. (2005) The classification of granitic pegmatites revisited. *Canadian Mineralogist* **43**, 2005–2026.

ČERNÝ, P., SELWAY, J.B., ERCIT, T.S., BREAKS, F.W., ANDERSON, A.J., & ANDERSON, S.D. (1998) Graftonite-beusite in granitic pegmatites of the Superior Province: a study in contrast. *Canadian Mineralogist* **36**, 367–376.

CORREIA NEVES, L.M. & LOPES NUNES, J.E. (1968) Pegmatitic phosphates of Alto-Ligonha region (Mozambique – Portuguese East Africa). *Revista de Ciência Geológicas Lourenço Marques* **1A**, 1–48.

DANA, J.D. & DANA, E.S. (1892) *The system of mineralogy*, *6th edition*. Wiley and Sons, New York-London.

EAKINS, L.G. (1891) Triplite. *United States Geological Survey Bulletin* **60**, 135.

FARRUGIA, L.J. (1999) WinGX suite for small-molecule single-crystal crystallography. *Journal of Applied Crystallography* **32**, 837–838.

FORNASERI, M. (1944) Sulla probabile identità della arrojadite con la triplite. *Periodico di Mineralogia* **14**, 35–41.

FRANSOLET, A.M., KELLER, P., & FONTAN, F. (1986) The phosphate mineral associations of the Tsaobismund pegmatite, Namibia. *Contributions to Mineralogy and Petrology* **92**, 502–517.

FUCHS, J.N. (1839) Ueber ein einfaches Verfahren, den Eisengehalt der Eisenerze so wie anderer eisenhaltiger Körper zu bestimmen und das Verhältniss von Eisenoxyd und Eisenoxydul darin auszumitteln; nebst Bemerkungen über ein Eisenphosphat von Rabenstein bei Bodenmais. *Journal für Praktische Chemie* **17**, 160–173.

GATTA, G.D., NESTOLA, F., BROMILEY, G.D., & LOOSE A. (2006a) New insight into crystal chemistry of topaz: A multi-methodological study. *American Mineralogist* **91**, 1839–1846.

GATTA, G.D., NESTOLA, F., & BOFFA BALLARAN, T. (2006b) Elastic behaviour and structural evolution of topaz at high pressure. *Physics and Chemistry of Minerals* **33**, 235–242.

GROAT, L.A., MULJA, T., MAUTHNER, M.H.F., ERCIT, T.S., RAUDSEPP, M., GAULT, R.A., & ROLLO, H.A. (2004) Geology and mineralogy of the Little Nahanni rare-element granitic pegmatites, Northwestern Territories. *Canadian Mineralogist* **41**, 139–160.

GUASTONI, A. (2012) *LCT and NYF pegmatites in the central Alps. Proxies of exhumation history of the Alpine nappe stack in the Lepontine Dome*. Ph.D. thesis, University of Padova, Padova, Italy.

HAMBERG, A. (1904) Ein Vorkommen von Triplit und ungewöhnlich grossen Turmalinen bei Skrumpetorp im Kirchspiel Godegard in Östergötland. *Geologiska Föreningen i Stockholm Förhandlingar* **26**, 77–86.

HAUSMANN, J.F.L. (1813) *Handbuch der Mineralogie*, *1st edition*. Göttingen.

HEINRICH, E.W. (1951) Mineralogy of triplite. *American Mineralogist* **36**, 256–271.

HENDERSON, E.P. (1933) Triplite from La Rioja Province, Argentina. *American Mineralogist* **18**, 104–105.

HESS, F.L. & HUNT, W.F. (1913) Triplite from Eastern Nevada. *American Journal of Sciences* **36**, 51–54.

HURLBUT, C.S. (1936) A new phosphate, bermanite, occurring with triplite in Arizona. *American Mineralogist* **21**, 656–661.

DE JESUS, A.M. (1933) Pegmatites mangano-litiníferas da região de Mangualde. *Comunicações dos Serviços Geológicos de Portugal* **19**, 65–210.

JOHN, C.V. (1900) Über einige neue Mineralvorkommen aus Mähren. *Verhandlungen der Kaiserlich-Königlichen Geologischen Reichsanstalt* **50**, 335–341.

KELLER, P. & VON KNORRING, O. (1989) Pegmatites at the Okatjimukuju farm, Karibib, Namibia Part I: Phosphate mineral associations of the Clementine II pegmatite. *European Journal of Mineralogy* **1**, 567–593.

KELLER, P., FRANSOLET, A.M., & FONTAN, F. (1994) Triphylite – lithiophilite and triplite – zwieselite in granitic pegmatites: Their textures and genetic relationships. *Neues Jahrbuch für Mineralogie Abhandlungen* **168**, 127–145.

VON KOBELL, W.F. (1864) Üeber die quantitative Bestimmung des Fluors in Eisen- Mangan- Phosphaten und Analyse des Triplit von Schlaggenwald in Böhmen. *Journal für Praktische Chemie* **92**, 385–393.

KOVAR, F. & SLAVIK, F. (1900) Über triplit von Wien und Cyrillhof in Mähren und seine Zersetzungsprodukte. *Verhandlungen der Kaiserlich-Königlichen Geologischen Reichsanstalt,* 387–404.

KUNZ, G.F. (1884) Topaz and associated minerals at Stoneham, Maine. *American Journal of Science* **27**, 212–216.

LARSON, A.C. (1967) Inclusion of secondary extinction in least-squares calculations. *Acta Crystallographica* **23**, 664–665.

LAUBMANN, H. & STEIMNETZ, H. (1920) Phosphatfhürende Pegmatite des Oberpfälzer und Bayerischen Waldes. *Zeitschrift für Kristallographie* **55**, 523–586.

LOTTERMOSER, B.G. & LU, J. (1997) Petrogenesis of rare-element pegmatites in the Olary Block, South Australia, part 1. Mineralogy and chemical evolution. *Mineralogy and Petrology* **59**, 1–19.

MASON, B. (1941) Minerals of the Varuträsk pegmatite. XXII. triplite and vivianite. *Geologiska Föreningen i Stockholm Förhandlingar* **63**, 285–288.

NORDENSKJÖLD, L. (1902) Analys af Triplit från Lilla Elgsjöbröttet. *Geologiska Föreningen i Stockholm Förhandlingar* **24**, 412–414.

OTTO, H. (1936) Die rolle des mangans in den mineralien. *Mineralogische und Petrographische Mitteilungen* **47**, 89–140.

OXFORD DIFFRACTION (2010) Xcalibur CCD system, CrysAlis Software system. Oxford Diffraction, Oxford, England.

PEHRMAN, G. (1939) Über Phosphate aus dem Pegmatit von Lemnäs, Kimito, S.-W. Finnland. *Acta Academiae Aboensis mathematica et physica* **12**, 437–453.

REA, J.R. & KOSTINER, E. (1972) The crystal structure of manganese fluorophosphates, $Mn_2(PO_4)F$. *Acta Crystallographica* **B28**, 2525-2529.

RODA, E., FONTAN, F., PESQUERA, A., & VELASCO, F. (1996) The phosphate mineral association of the granitic pegmatites of the Fregeneda area (Salamanca, Spain). *Mineralogical Magazine* **60**, 767-778.

RODA, E., PESQUERA, A., FONTAN, F., & KELLER, P. (2004) Phosphate mineral associations in the Cañada pegmatite (Salamanca, Spain): Paragenetic relationships, chemical compositions, and implications for pegmatite evolution. *American Mineralogist* **89**, 110–125.

SCHMID, S.M., BERGER, A., DAVIDSON, C., GIERÉ, R., HERMANN, J., NIEVERGELT, P., PUSCHNIG, A.R., & ROSEMBERG, A. (1996) The Bergell pluton (South Switzerland, Northern Italy): overview accompanying a geological-tectonic map of the intrusion and surrounding country rocks. *Schweizerische Mineralogische und Petrographische Mitteilungen* **76**, 329–355.

SEJKORA, J., ŠKODA, R., ONDRUŠ, P., BERAN, P., & SÜSSER, C. (2006) Mineralogy of phosphate accumulation in the Huber stock, Krásno ore district, Slavkovský les area, Czech Republic. *Journal of the Czech Geological Society* **51**, 103–147.

SELLNER, F. (1924) Die Pegmatite der Umgebung von Marienbad. *Zeitschrift für Kristallographie* **60**, 275–277.

SHAININ, V.E. (1946) The Branchville, Connecticut, pegmatite. *American Mineralogist* **31**, 329–345.

SHANNON, E.V. (1920) Notes on anglesite, anthophyllite, calcite, datolite, sillimanite, stilpnomelane, tetrahedrite and triplite. *Proceedings of the United States National Museum* **58**, 437–453.

SHELDRICK, G.M. (1997) SHELX-97. Programs for crystal structure determination and refinement. University of Göttingen, Germany.

SIMMONS, W.B., WEBBER, K.L., FALSTER, A.U., & NIZAMOFF J.W. (2003) *Pegmatology: pegmatite mineralogy, petrology & petrogenesis*. Rubellite Press, New Orleans, 176.

STELZNER, A. (1873) Mineralogische Beobactungen im Gebeite der Argentinischen Republik. *Mineralogische und Petrographische Mitteilungen* **23**, 227–254.

VAUQUELIN, L.N. (1802) Phosphate natif de fer melangé de manganèse. *Journal des Mines* **11**, 295.

WALDROP, L. (1969) The crystal structure of triplite, $(Mn,Fe)_2FPO_4$. *Zeitschrift für Kristallographie* **130**, 1–14.

WALDROP, L. (1970) The crystal structure of triploidite and its relation to the structures of other minerals of the triplite-triploidite group. *Zeitschrift für Kristallographie* **131**, 1–20.

WALLACE, R.E. (1940) Crystal chemistry of the phosphates, arsenates and vanadates of the type $A_2XO_4(Z)$. *American Mineralogist* **25**, 441–479.

WOLFE, C.W. & HEINRICH, E.W. (1947) Triplite crystals from Colorado. *American Mineralogist* **32**, 518–526.

Received June 12, 2013. Revised manuscript accepted March 17, 2014.